VENTILATION FLOW IN A BAROCLINIC VORTEX RELATED TO TROPICAL CYCLONE MOTION*

Tian Yongxiang (田永祥)

Nanjing Institute of Meteorology, Nanjing 210044

Received March 15, 1995

ABSTRACT

The tropical cyclone motion is numerically simulated with a quasi-geostrophic baroclinic model. The flow field of a tropical cyclone is decomposed into its axisymmetric and asymmetric components. The relation between the ventilation flow vector and the motion vector of the tropical cyclone is investigated. The results of numerical experiments indicate: (1) There are both large-scale beta gyres and small-scale gyres in the asymmetric flow field. (2) The interaction between small-scale gyres and large-scale beta gyres leads to the oscillation of translation speed and translation direction for the tropical cyclone. (3) There are the large deviations between the ventilation flow vector calculated by means of Fiorino and Elsberry's method and the motion vector of tropical cyclone. (4) The ventilation flow vector computed using the improved method closely correlates with the motion vector of the tropical cyclone.

Key words: tropical cyclone, large-scale beta gyres, small-scale gyres, ventilation flow, motion

I. INTRODUCTION

In the mid 1980s, Chen (1985) suggested that the tropical cyclone structure was an important factor influencing its translation. Later, Chan and Williams (1987), Fiorino and Elsberry (1989), Li and Zhu (1990) investigated how the tropical cyclone structure affects its translation with analytical and/or numerical models. It should be specially pointed out that Fiorino and Elsberry (1989) numerically simulated tropical cyclone motion with a quasi-geostrophic barotropic model and decomposed the total streamfunction into its axisymmetric and asymmetric components. They discovered that the ventilation flow vector determined by the large-scale beta gyres in the asymmetric flow field was closely correlated with the motion vector of the tropical cyclone. Nevertheless, the tropical cyclone simulated by Fiorono and Elsberry only moved toward the northwest in a uniform acceleration.

Tian and Luo (1994), Tian (1994; 1995) numerically simulated the tropical cyclone motion with a quasi-geostrophic baroclinic model. The results indcated that there were both the large-scale beta gyres and the small-scale gyres in the asymmetric flow field of the model tropical cyclone; and that the translation speed and direction of tropical cyclone appeared obviously oscillatory and vacillating.

The primary goal of this research is to further clarify the following:

* This work is supported by the 8th Five-Year Project of Key Item Research of China under Grant 85-906-07-02-04.

(1) How the small-scale gyres affect the tropical cyclone motion.

(2) Whether or not the correlation between ventilation flow vector calculated by means of Fiorino and Elsberry' s method and the motion vector of the tropical cyclone would still be close if the influence of small-scale gyres is involved.

(3) How the method of computing the ventilation flow vector should be improved if the above correlation weakens.

II. NUMERICAL MODEL

We assume that $p_0 = 100$ hPa and $p_6 = 1000$ hPa are the upper and lower boundaries of the model atmosphere. respectively. And the model atmosphere is equally divided into three discrete layers with the pressure interval being $\Delta p = 300$ hPa (Fig. 1).

We apply the vorticity equation at the model levels 1, 3 and 5, and the adiabatic thermodynamic equation for the model levels 2 and 4. Assuming the basic flow to be zero, we derive the closed equations for the quasi-geostrophic three-layer model from the above equations. i. e.

$$\frac{\partial}{\partial t}\nabla^2\psi_k = -J(\psi_k, \nabla^2\psi_k) - \beta\frac{\partial\psi_k}{\partial X} + \frac{f_0}{\Delta p}(\omega_{k+1} - \omega_{k-1}), \qquad (k = 1, 3, 5) \tag{1}$$

$$\nabla^2\omega_k - \frac{f_0^2}{\sigma_k(\Delta p)^2}(2\omega_k - \omega_l) = \frac{f_0}{\sigma_k\Delta p}\{-J(\psi_{k-1}, \nabla^2\psi_{k-1}) + J(\psi_{k+1}, \nabla^2\psi_{k+1}) - \beta\left(\frac{\partial\psi_{k-1}}{\partial X} - \frac{\partial\psi_{k+1}}{\partial X}\right) + \nabla^2[J(\psi_k, \psi_{k-1} - \psi_{k+1})]\}, \qquad (k = 2, 4) \tag{2}$$

where the dependent variables ψ_k and ω_k are the pertubation streamfunction (called streamfunction for short) and the vertical velocity respectively, σ_k the static stability parameter. In Eq. (2), we specify $\omega_l = \omega_{k+2}$ for $k = 2$, and $\omega_l = \omega_{k-2}$ for $k=4$.

At the model level 3 (i. e. 550 hPa), the initial vorticity profile of model tropical cyclone (Chan 1987) is given by

$$\zeta_3(r) = \frac{2V_m}{r_m}[1 - \frac{1}{2}(\frac{r}{r_m})^b]\exp\{\frac{1}{b}[1 - (\frac{r}{r_m})^b]\}, \tag{3}$$

where $r = \sqrt{(x - x_0)^2 + (y - y_0)^2}$ is the radius, (x_0, y_0) the coordinates of the tropical cyclone centre, V_m the maximum wind speed, r_m the radius of maximum wind, and b the factor that determines the shape of vortex. Solving the Poisson equation

$$\nabla^2\psi_3(x, y) = \zeta_3(x, y) \tag{4}$$

from $\zeta_3(x, y)$, we obtain the initial streamfunction profile $\psi_3(x, y)$. Referring to the vertical profile of streamfunction for the tropical cyclone given by Kitade (1980), we specify the initial streamfunction profiles at the model levels 1 (250 hPa) and 5 (850 hPa) to be

$$\begin{aligned} \psi_1(x, y) &= C_1\psi_3(x, y), \\ \psi_5(x, y) &= C_5\psi_3(x, y), \end{aligned} \tag{5}$$

respectively.

The domain of the numerical experiments is an east-west zonal area with 51×51 points. The grid spacing is uniform with a horizontial grid spacing of 50 km. The horizontial lateral boundary conditions are $\psi_k = 0$ along the northern and southern boundaries of the zone and the cyclic continuity in the east-west direction. The following vertical boundary conditions are adopted:

$$\omega_0 = 0 \quad \text{at } p_0 = 100 \text{ hPa},$$
$$\omega_6 = 0 \quad \text{at } p_6 = 1000 \text{ hPa}. \tag{6}$$

The Jacobian terms of the model equations (1) and (2) are evaluated using the finite difference format developed by Arakawa (1966). The model equations are solved by means of the super-relaxation iteration method. The time step of numerical integration is 10 min. The total integrating time is 4 model days.

The model parameters are chosen as follows: $\sigma_k = 0.032$ m^2 s^{-2} hPa^{-2} for $k = 2, 4$, $\beta = 2.0746 \times 10^{-11}$ m^{-1} s^{-1}; $V_m = 25$ m s^{-1} (at the model level 3), $r_m = 100$ km, $b = 1$; $C_1 = 0.3$, $C_5 = 1.5$.

III. EFFECT OF SMALL-SCALE GYRES ON TROPICAL CYCLONE MOTION

In this study, we decompose the total streamfunction $\psi_k(x, y, t)$ into an axisymmetric component $\psi_{ks}(x, y, t)$ and an asymmetric one $\psi_{ka}(x, y, t)$.

From Fig. 2 we can see that there are the large-scale beta gyres (LSBGs) in the asymmetric flow fields at various model levels. The distance d_l between the two centres of LSBG depends on altitude. They are 939, 932 and 467 km at 850, 550 and 250 hPa, respectively. The intensities of LSBG weaken with height.

In the asymmetric flow fields at 850 and 550 hPa, the small-scale gyres (SSGs) occur near the tropical cyclone centres. The distances d_s between the two centres of SSG are 228 and 162 km at 850 and 550 hPa, respectively. The SSGs are stronger than the LSBGs at 850 hPa. The intensities of SSGs are equivalent to those of LSBGs at 550 hPa. The SSGs rotate around the tropical cyclone centres counterclockwise. The existence of SSGs was confirmed by Marks et al. (1992) from the detection.

Tian (1995) studies the physical mechanism of SSGs formation with the aid of streamfunction tendency analysis. The results indicate that the linear beta effect produces LSBGs and provides a background condition for the formation of SSGs; and that the nonlinear effect, i. e. the advection of asymmetric vorticity by symmetric flow creates SSGs.

In all the 4 model days, there are always SSGs at 550 hPa. During hour 16 — 25, 31—42, 53—64 and 84—90, the azimuthal phase differences (APD) between SSG and LSBG exist. During hour 26—30, 43—52 and 65—83, the SSGs tend to coincide with the LSBGs.

As shown in Fig. 3 and Fig. 4, the translation speed of tropical cyclone V_c at 550 hPa obviously oscillates with time. In the 4 model days, the four accelerated and four decelerated motion processes occur. When the APD between SSG and LSBG exists, the V_c slows down. While the SSGs tend to coincide with the LSBGs, the V_c speeds up.

The translation direction of tropical cyclone θ_c at 550 hPa evidently vacillates with time (Fig. 3 and Fig. 5). In the 4 model days, the two marked direction change processes appear. The first direction change occurs in hour 32—42 and the θ_c changes from the northwest by west to the southwest, the east, the northeast and the north northwest, and the V_c slows down (Table 1). The second direction change occurs in hour 55—65. The θ_c changes from the northwest by west to the north northeast, and the V_c slows down also (Table 1). During the direction change of the tropical cyclone, the APD between SSG and LSBG exists. Thus, it can be seen that the existance of APD between SSG and LSBG is a necessary condition for the direction change of tropical cyclones.

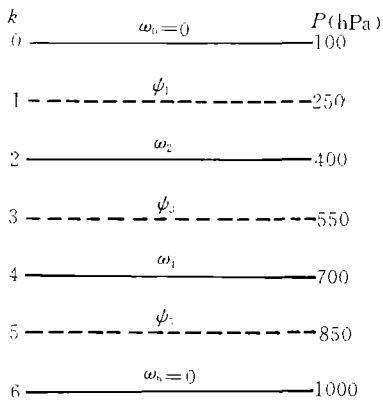

Fig. 1. The arrangement of variables in the vertical for the quasi-geostrophic three-layer model.

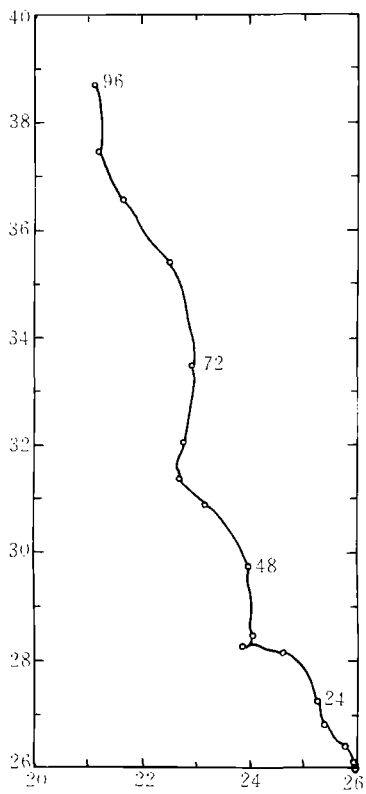

Fig. 3. The tropical cyclone track at 550 hPa. The symbols along the track are 6 h apart. The graduated intervals on the figure frames are 50 km.

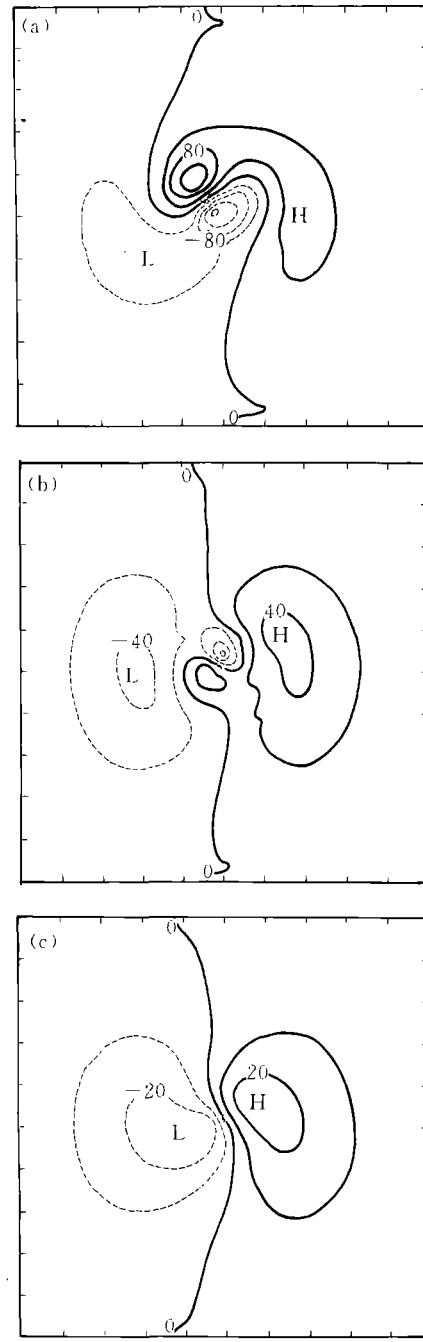

Fig. 2. The asymmetric streamfunction ψ_a at 24 h on (a) 850 hPa, (b) 550 hPa and (c) 250 hPa. The contour intervals are 40, 20 and 10 (10^4 m^2 s^{-1}) respectively. The graduated intervals on the figure frames are 250 km.

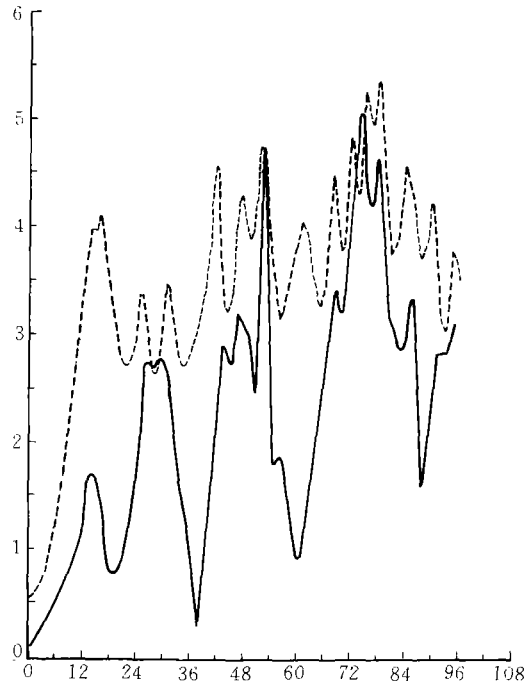

Fig. 4. The temporal variation of the translation speed for tropical cyclone V_c (solid, m s^{-1}) and the ventilation flow speed calculated by Fiorino and Elsberry's method V_f (dashed, m s^{-1}) at 550 hPa.

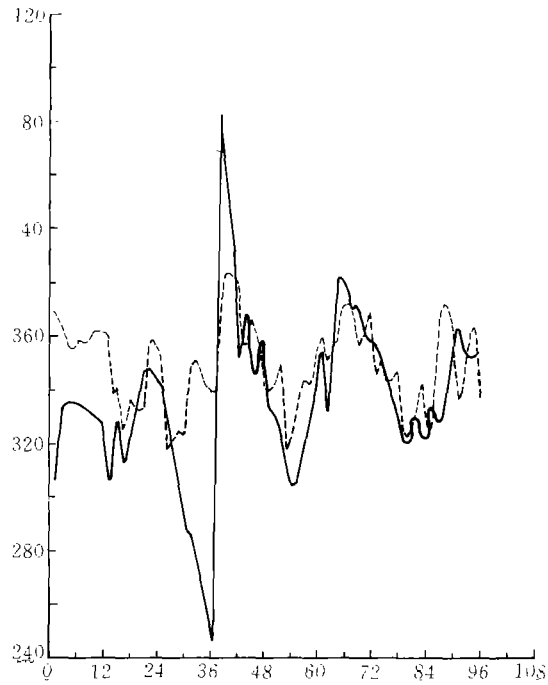

Fig. 5. The temporal variation of the translation direction for tropical cyclone θ_c (solid, in °) and the ventilation flow direction calculated by the method of Fiorino and Elsberry θ_f (dashed, in °) at 550 hPa.

Table 1. The Temporal Variation of the Translation Speed V_c and the Translation Direction θ_c for Tropical Cyclone at 550 hPa

t (h)	V_c (m s^{-1})	θ_c (°)	t (h)	V_c (m s^{-1})	θ_c (°)
31	2.6	287	54	1.7	304
32	2.1	288	55	1.8	303
33	1.6	279	56	1.9	311
34	1.4	267	57	1.8	319
35	1.1	259	58	1.5	325
36	0.8	254	59	1.1	333
37	0.3	242	60	0.9	346
38	0.2	95	61	0.9	359
39	0.7	69	62	1.4	326
40	1.2	52	63	1.7	343
41	1.7	39	64	2.1	22
42	2.3	354	65	2.4	22

IV. RELATION BETWEEN VENTILATION FLOW CALCULATED BY FIORINO AND ELSBERRY'S METHOD AND TROPICAL CYCLONE MOTION

The results of Fiorino and Elsberry (1989) indicated that the ventilation flow vector between large-scale cyclonic and anticyclonic beta gyres in the asymmetric flow field was closely correlated with the motion vector of the tropical cyclone. Now, the procedure of calculating the ventilation flow vector developed by them is outlined as follows.

(1) A circular area A_k at a radius (r) of 300 km around the tropical cyclone centre is chosen.

(2) The asymmetric wind speed components $u_{ka}(x, y, t)$ and $v_{ka}(x, y, t)$ at all the model grid points within the A_k are calculated by

$$u_{ka} = -\frac{\partial \psi_{ka}}{\partial y}, \qquad v_{ka} = \frac{\partial \psi_{ka}}{\partial x} \tag{7}$$

respectively.

(3) The asymmetric wind speed $V_{ka}(x, y, t)$ and wind direction $\theta_{ka}(x, y, t)$ are computed by using

$$V_{ka} = \sqrt{u_{ka}^2 + v_{ka}^2}, \qquad \theta_{ka} = \mathrm{tg}^{-1}(v_{ka}/u_{ka}) \tag{8}$$

respectively.

(4) The ventilation flow speed $V_{kf}(t)$ and direction $\theta_{kf}(t)$ are obtained by algebraically averaging $V_{ka}(x, y, t)$ and $\theta_{ka}(x, y, t)$ in the A_k, respectively.

When the APD between SSG and LSBG exists (t=16—25 h, 31—42 h, 53—64 h and 84—90 h), the ventilation flow speed calculated by Fiorono and Elsberry's method V_f is 2—3 m s^{-1} larger than the translation speed of tropical cyclone V_c (Fig. 4), and the deviations between the ventilation flow direction θ_f and the translation direction of tropical cyclone θ_c are large (Fig. 5). While the SSGs tend to coincide with the LSBGs (t=26—30 h, 43—52 h and 65—83 h), the V_f is close to the V_c, and the θ_f approaches the θ_c.

The reason causing the deviations between the ventilation flow vector and the motion vector of the tropical cyclone is that the effect of SSGs is considered insufficiently in Fiorino and Elsberry's method. When the APD between SSG and LSBG exists, the ventilation flow between two large-scale beta gyres is no longer uniform. Under this circumstances, it is not appropriate to calculate the ventilation flow vector by the algebraical average method in the A_k. Therefore, it is necessary to improve the method of calculating the ventilation flow vector.

V. RELATION BETWEEN VENTILATION FLOW COMPUTED USING AN IMPROVED METHOD AND TROPICAL CYCLONE MOTION

In order to sufficiently consider the effect of SSGs on the tropical cyclone motion, we have advanced a method of computing the ventilation flow vector. Its computational procedure is briefly described as follows.

(1) Choosing a circular area A_k.

(2) Calculating the asymmetric wind speed components $u_{ka}(x, y, t)$ and $v_{ka}(x, y, t)$ at all the model grid points within the A_k using Eq. (7).

(3) Averaging the $u_{ka}(x, y, t)$ and $v_{ka}(x, y, t)$ in the A_k respectively, and then obtaining

the $\bar{u}_{ka}(t)$ and $\bar{v}_{ka}(t)$.

(4) Computing the ventilation flow speed $V_{ki}(t)$ and direction $\theta_{ki}(t)$

$$V_{ki} = \sqrt{\bar{u}_{ka}^2 + \bar{v}_{ka}^2}, \qquad \theta_{ki} = \mathrm{tg}^{-1}(\bar{v}_{ka}/\bar{u}_{ka}) \tag{9}$$

respectively.

From Fig. 6 and Fig. 7 we can see that whether the SSGs tend to coincide with the LSBGs or the APD between them exists, the ventilation flow speed V_i and direction θ_i are closely correlated to the translation speed V_c and direction θ_c of tropical cyclone, respectively. The four accelerated and four decelerated motion processes and the two direction change processes for the model tropical cyclone can be all reflected from the variations of V_i and θ_i with time, respectively. Thus, it can be said that the ventilation flow computed using the improved method steers the movement of the tropical cyclone.

Owing to variations of intensity and horizontal scale of the SSGs and the LSBGs with height, a different circular area A_k at various model levels should be chosen to calculate the ventilation flow vector. We have chosen seven kinds of circular areas A_k (r=200—500 km, Δr= 50 km) at each model level. We adopt the 95 samples (one sample is chosen once every hour from hour 1 to hour 95) to compute the correlation coefficients between the ventilation flow vector (V_i, θ_i) and the motion vector of tropical cyclone (V_c, θ_c) for each circular area A_k.

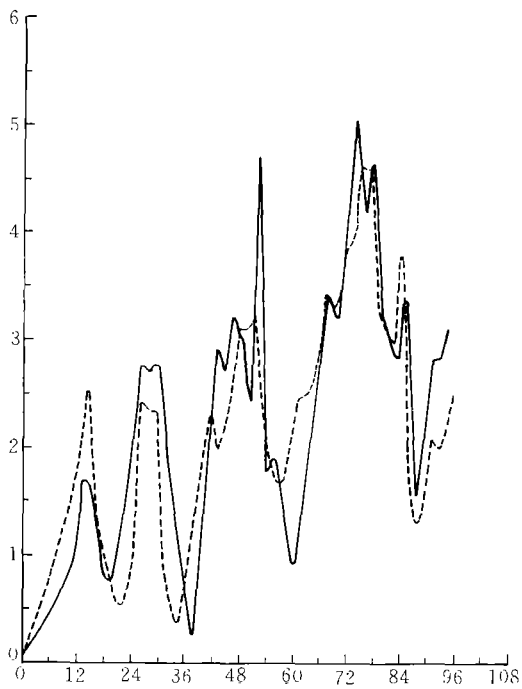

Fig. 6. The temporal variation of the translation speed for tropical cyclone V_c (solid, m s^{-1}) and the ventilation flow speed computed using the improved method V_i (dashed, m s^{-1}) at 550 hPa.

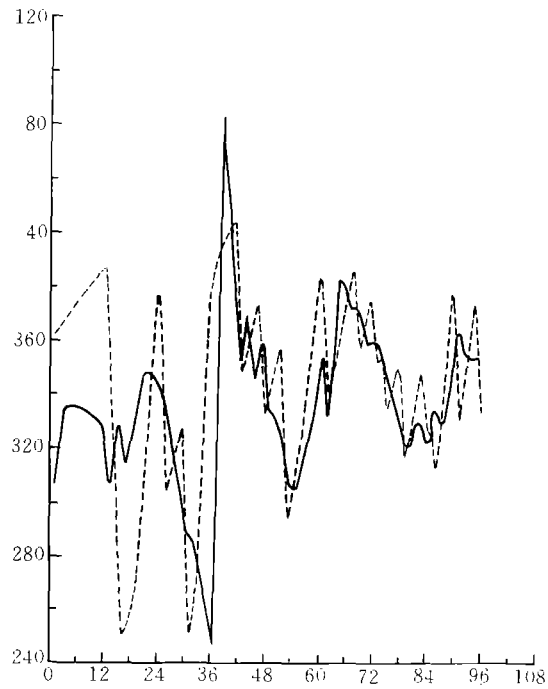

Fig. 7. The temporal variation of the translation direction for tropical cyclone θ_c (solid, in°) and the ventilation flow direction computed using the improved method θ_i (dashed, in°) at 550 hPa.

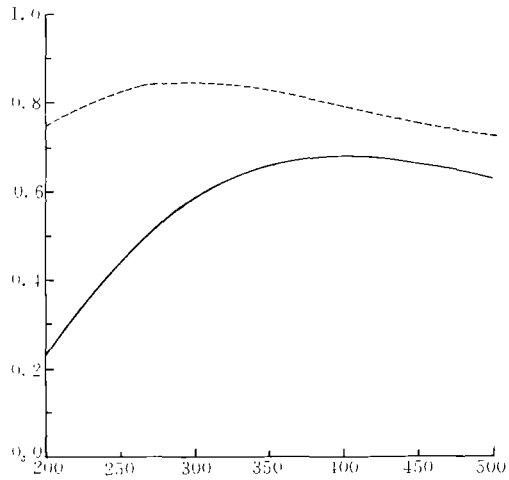

Fig. 8. The variation of the speed correlation coefficients $(R_v)_{850}$ (solid) and $(R_v)_{550}$ (dashed) with circular areas at a radius of r (km) at 850 and 550 hPa.

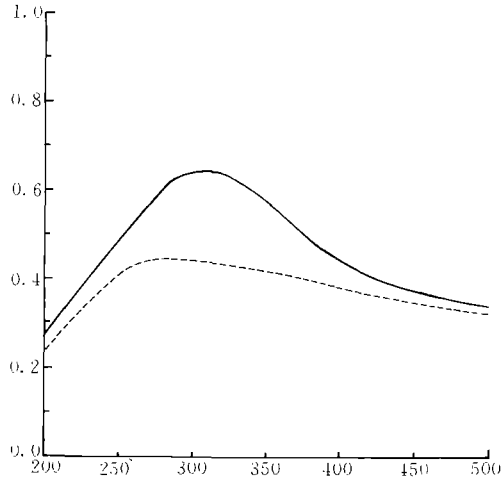

Fig. 9. The variation of the direction correlation coefficients $(R_\theta)_{850}$ (solid) and $(R_\theta)_{550}$ (dashed) with circular areas at a radius of r (km) at 850 and 550 hPa.

At 850 hPa, the best correlation scale r_b is 300—400 km. The corresponding speed correlation coefficient $(R_v)_{850}$ is equivalent to the direction correlation coefficient $(R_\theta)_{850}$ (Fig. 8, Fig. 9 and Table 2). At 550 hPa, the best correlation scale r_b is 300 km. Nevertheless, the $(R_v)_{550}$ is obviously superior to the $(R_\theta)_{550}$.

Table 2. The Best Correlation Scale r_b and the Corresponding Correlation Coefficients R_v and R_θ

Level (hPa)	Speed correlation		Direction correlation	
	r_b (km)	R_v	r_b (km)	R_θ
850	400	0.68	300	0.68
550	300	0.85	300	0.45

From the above analysis we can know that the ventilation flow in circular areas with radiuses (r) being 300—400 km around the centre controls the motion of the model tropical cyclone.

VI. VENTILATION FLOW CALCULATED USING ACTUAL DATA RELATED TO TYPHOON MOTION

In the period of SPECTRUM-90, the target typhoon Yancy (9012) was to the southeast of Taiwan (i. e. 20. 8°N, 124. 5°E) at 0000 GMT 19 August. Later, it moved toward the nouthwest in a speed of 12. 5 m s^{-1}. At 1200 GMT 19 August, the Yancy lay near Taibei. Then, it turned to the west, and translation speed obviously slowed down (4. 2 m s^{-1}). At 0000 GMT 20 August, the Yancy was located to the east of Quanzhou, Fujian Province, about 100 km apart. Then, it turned to the southwest by west, and the translation speed 4. 2 m s^{-1} kept unchanged. At 1200 GMT 20 August, the Yancy was situated in the vicinity of

Xiamen.

We have calculated the ventilation flow vectors at 500 hPa from 19 to 20 August using the two methods (Table 3).

Table 3. The Ventilation Flow Vectors at 500 hPa of the Target Typhoon Yancy (9012) Compared with Its Motion Vector

t / θ_c / θ_i / r	t_1	t_2	t_3	t / V_c / V_i / r	t_1	t_2	t_3
	326	276	239		12.5	4.2	4.2
400	34	280	234	400	13.0	16.7	12.2
500	22	278	236	500	7.4	11.9	10.0
600	16	273	243	600	6.9	9.8	7.9
700	10	270	249	700	6.1	8.4	5.7
800	357	270	256	800	5.3	6.8	3.4
t / θ_f / r	t_1	t_2	t_3	t / V_f / r	t_1	t_2	t_3
400	11	290	247	400	25.8	20.3	14.8
500	358	309	272	500	25.6	18.2	14.2
600	2	310	285	600	23.5	16.8	13.7
700	358	311	301	700	21.7	15.2	13.5
800	352	312	313	800	20.3	13.7	13.5

Note: The θ_c, θ_i and θ_f are in a unit of degree. The V_c, V_i and V_f are in a unit of m s^{-1}. The r is in a unit of km. The t_1, t_2 and t_3 represent 0000 GMT 19 August, 1200 GMT 19 August and 0000 GMT 20 August, respectively.

First, we analyse the ventilation flow vector computed using the improved method (V_i, θ_i) related to the motion vector of typhoon Yancy (V_c, θ_c). At 0000 GMT 19 August, the θ_i pointed to the northeast by north or to the north. There were certain deviations between θ_i and θ_c. The V_i calculated in the circular areas with radiuses $r=400-500$ km was closer to the V_c. At 1200 GMT 19 August, the θ_i pointed to the west and was consistent with the θ_c. From Fig. 10b we can see that the ventilation flow near the centre of typhoon Yancy steered the typhoon moving toward the west. At 0000 GMT 20 August, the θ_i pointed to the southwest by west, still was in accordance with the θ_c. It should be pointed out, when the typhoon Yancy approached the continent of China, the V_i calculated in a large circular area ($r=800$ km) became closer to the V_c.

Second, we analyse the ventilation flow vector calculated by Fiorino and Elsberry's method (V_f, θ_f) related to the motion vector of typhoon Yancy (V_c, θ_c). Except the θ_f was closer to the θ_c at 0000 GMT 19 August, there were the large deviations between the θ_f and the θ_c at the other time. At any time, the V_f was markedly larger than the V_c.

The above analysed results of the actual data indicate that the ventilation flow vector computed using the improved method more closely correlates to the motion vector of the typhoon. Therefore, we can regard the ventilation flow vector computed using the improved method as a reference index for forecasting typhoon tracks.

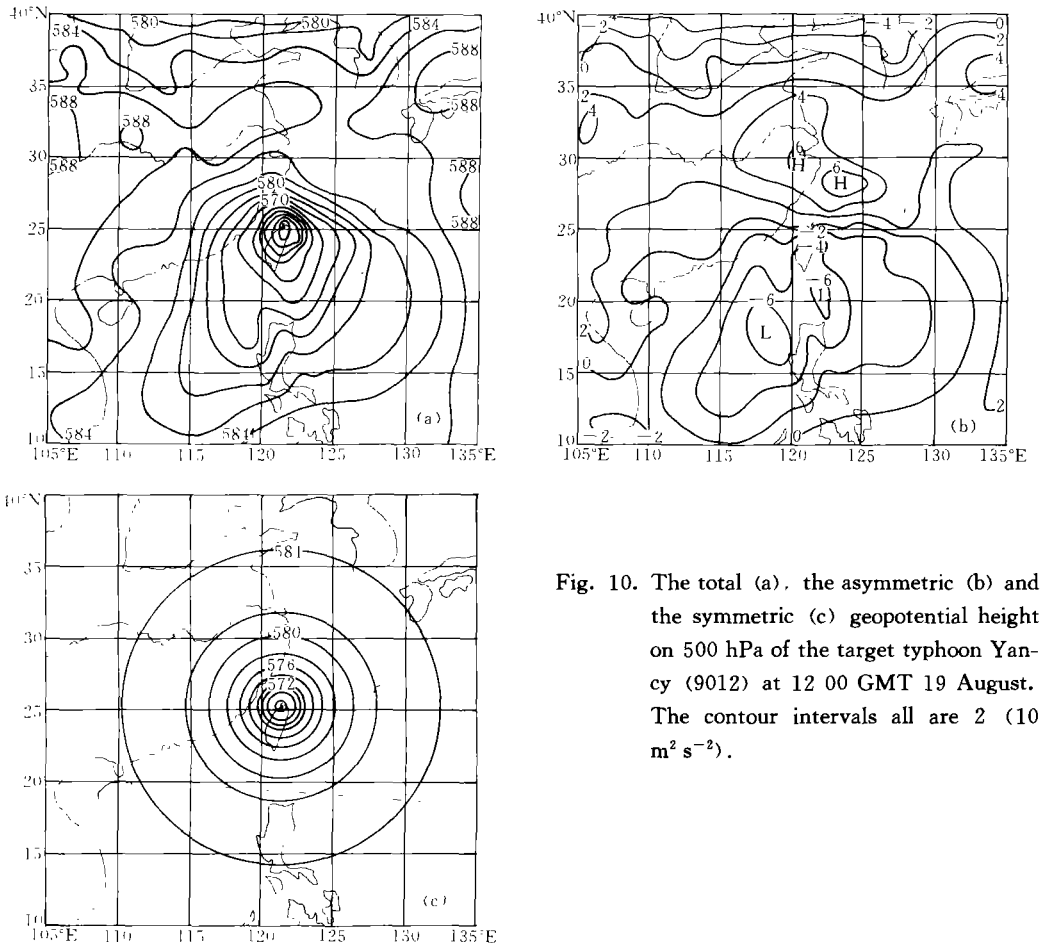

Fig. 10. The total (a), the asymmetric (b) and the symmetric (c) geopotential height on 500 hPa of the target typhoon Yancy (9012) at 12 00 GMT 19 August. The contour intervals all are 2 (10 $m^2 s^{-2}$).

VII. CONCLUSION AND DISCUSSION

To sum up, we can come to the following conclusion.

(1) Numerically simulating the tropical cyclone motion with a quasi-geostrophic baroclinic model, we find that there are both large-scale beta gyres and the small-scale gyres in the asymmetric flow field. The linear beta effect produces the large-scale beta gyres and provides a background condition for the formation of small-scale gyres. The nonlinear effect, i. e. the advection of asymmetric vorticity by symmetric flow, creates the small-scale gyres.

(2) The interaction of the small-scale gyres with the large-scale beta gyres leads to the oscillation of translation speed and the vacillation of translation direction for a baroclinic tropical cyclone.

(3) When the azimuthal phase differences between the small-scale gyres and the large-scale beta gyres exist, there are the large deviations between the ventilation flow vector calculated by Fiorino and Elsberry' s method and the motion vector of the tropical cyclone.

(4) In order to sufficiently consider the effect of small-scale gyres on tropical cyclone motion, we have advanced an improved method of computing the ventilation flow vector. The results calculated using the model and actual tropical cyclone data indicate that the ventilation flow vector computed using the improved method more closely correlates the motion vector of

tropical cyclone.

(5) For the given model tropical cyclone, it is the ventilation flow in circular areas with radii $r=300-400$ km around the centre that controls its motion.

The dynamics of tropical cyclone motion in a baroclinic atmosphere is quite complicated and involves many physical processes. The quasi-geostrophic model developed in this study is very simple, in which the basic flow is assumed to be zero, the moist physical process is not included, and vertical translations of various physical quantities are considered insufficiently. Therefore, the whole structure of tropical cyclone in the model atmosphere would be different from that in the actual atmosphere. If we improve the model further, it would be expected to gain better simulated results.

In the process of accomplishing this study, Prof. Luo Zhexian gives me warm guidance and help. Here, I wish to convey my hearty thanks to him.

REFERENCES

Arakawa, A. (1966), Computational design for long-term numerical integrations for the equations of atmospheric motion, *J. Comput. Physics*, **1**: 119—143.

Chan, J. C. L. and Williams, R. T. (1987), Analytical and numerical studies of the beta-effect in tropical cyclone motion. Part I : Zero mean flow, *J. Atmos. Sci.*, **44**: 1257—1265.

Chen Lianshou (1985), The current situation and development of studies on tropical cyclone motion and operational forecast, *Collected Works of Typhoon Conference*, China Meteor. Press, Beijing, pp. 6—30 (in Chinese).

Fiorino, M. and Elsberry, R. L. (1989), Some aspects of vortex structure related to tropical cyclone motion, *J. Atmos. Sci.*, **46**: 975—990.

Kitade, T. (1980), Numerical experiments of tropical cyclones on a plane with variable Coriolis parameter, *J. Meteor. Soc. Japan*, **58**: 471—487.

Li Tianming and Zhu Yongti (1990), Analysis and simulation of tropical cyclone motion. Part I : Non-axisymmetric structure and abrupt change of path, *Sci. Sinica (Ser. B)*, **1**: 104—112 (in Chinese).

Marks, F. D., Houze, R. A. and Gamache, J. F. (1992), Dual-aircraft investigation of the inner core of hurricane Norbert. Part I : Kinematic structure, *J. Atmos. Sci.*, **49**: 919—942.

Tian Yongxiang and Luo Zhexian (1994), Vertical structure of beta gyres and its effect on tropical cyclone motion, *Adv. Atmos. Sci.*, **11**: 43—50.

Tian Yongxiang (1994), The fine structure of asymmetric circulation and vacillation in typhoon track, *Journal of Nanjing Institute of Meteorology*, **17**: 399—404 (in Chinese).

Tian Yongxiang (1995), The formation of small-scale gyres and its effect on tropical cyclone motion, *Journal of Applied Meteorology*, (in Chinese, will be published in 1995).